# Impact of cancer-associated mutations in CC chemokine receptor 2 on receptor function and antagonism

Hollander, L.S. den; Béquignon, O.J.M.; Wang, X.; Wezel, K. van; Broekhuis, J.; Gorostiola González, M.; ... ; Heitman, L.H.

Biochemical Pharmacology 208 (2023) 115399

Contents lists available at ScienceDirect

Biochemical Pharmacology

journal homepage: www.elsevier.com/locate/biochempharm

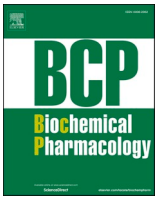

# Impact of cancer-associated mutations in CC chemokine receptor 2 on receptor function and antagonism

L.S. den Hollander [a], O.J.M. Béquignon [a], X. Wang [a], K. van Wezel [a], J. Broekhuis [a], M. Gorostiola González [a,b], K.E. de Visser [b,c,d], A.P. IJzerman [a], G.J.P. van Westen [a], L. H. Heitman [a,b,*]

[a] Leiden Academic Centre for Drug Research, Division of Drug Discovery and Safety, Leiden, The Netherlands
[b] Oncode Institute, Leiden, The Netherlands
[c] Netherlands Cancer Institute, Division of Tumor Biology & Immunology, Amsterdam, The Netherlands
[d] Leiden University, Department of Immunology, Medical Centre, Leiden, The Netherlands

ARTICLE INFO

*Keywords:*
CC chemokine receptor 2
Cancer
Mutation
Orthosteric and allosteric antagonists

ABSTRACT

CC chemokine receptor 2 (CCR2), a G protein-coupled receptor, plays a role in many cancer-related processes such as metastasis formation and immunosuppression. Since ~ 20 % of human cancers contain mutations in G protein-coupled receptors, ten cancer-associated CCR2 mutants obtained from the Genome Data Commons were investigated for their effect on receptor functionality and antagonist binding. Mutations were selected based on either their vicinity to CCR2's orthosteric or allosteric binding sites or their presence in conserved amino acid motifs. One of the mutant receptors, namely S101P$^{2.63}$ with a mutation near the orthosteric binding site, did not express on the cell surface. All other studied mutants showed a decrease in or a lack of G protein activation in response to the main endogenous CCR2 ligand CCL2, but no change in potency was observed. Furthermore, INCB3344 and LUF7482 were chosen as representative orthosteric and allosteric antagonists, respectively. No change in potency was observed in a functional assay, but mutations located at F116$^{3.28}$ impacted orthosteric antagonist binding significantly, while allosteric antagonist binding was abolished for L134Q$^{3.46}$ and D137N$^{3.49}$ mutants. As CC chemokine receptor 2 is an attractive drug target in cancer, the negative effect of these mutations on receptor functionality and drugability should be considered in the drug discovery process.

## 1. Introduction

In 2020, 19.3 million new cancer cases, and 10 million cancer deaths were estimated to have occurred worldwide [1]. Cancer is a diverse and multifaceted disease in which G protein-coupled receptors (GPCRs) play a role as drivers of al cancer promoting hallmarks [2]. Currently, 8 small molecules and antibodies targeting GPCRs have been approved by the FDA for use in the treatment of cancer, with many more in the clinical trial phase [3].

CC chemokine receptor 2 (CCR2) is expressed on macrophages, natural killer cells, and dendritic cells, among others [4]. Its function is to guide leukocytes to sites of inflammation, as well as during homeostatic circulation, in response to a gradient of several different chemokines, the main cognate ligand being CC chemokine ligand 2 (CCL2). CCR2 and other chemokine receptors are involved in many autoimmune and inflammatory diseases, including cancer [5]. Overexpression of CCL2 and/or CCR2 in cancer has been shown to be unfavourable for patient health and survival [6,7]. It is hypothesized that recruited monocytes and macrophages in response to tumour-produced CCL2 may kill tumour cells [8]. However, the CCL2-CCR2 signalling axis has also been implicated in tumour growth and proliferation, angiogenesis, metastasis and immunosuppression [6]. This makes CCR2 a promising target for cancer treatment and a number of clinical trials with receptor antagonists are therefore in progress [9,10]. Nevertheless, inhibiting CCR2 has proven to be difficult as no drugs have made it to the market yes, mostly due to lack of efficacy. One of the postulated reasons for this failure is a high local concentration of chemokines, as has been seen in various forms of cancer, such as breast, lung and gastric cancer [11–13], which outcompetes the drug binding to the same site at the receptor [14].

Recently, two CCR2 crystal structures have been solved, one of which showed two binding sites on the receptor [15,16]. The first one of these sites is the well-known orthosteric binding site, where chemokines

* Corresponding author.
*E-mail address:* l.h.heitman@lacdr.leidenuniv.nl (L.H. Heitman).

https://doi.org/10.1016/j.bcp.2022.115399
Received 14 October 2022; Received in revised form 19 December 2022; Accepted 21 December 2022
Available online 26 December 2022

**Abbreviations**

| | |
|---|---|
| BCA | bicinchoninic acid |
| BSA | bovine serum albumin |
| CCL2 | CC chemokine ligand 2 |
| CCR2 | CC chemokine receptor 2 |
| DMEM | Dulbecco's Modified Eagle Medium |
| dNTP | deoxyribonucleotide triphosphate |
| ECL | extracellular loop |
| GDC | Genomic Data Commons |
| GPCR | G protein-coupled receptor |
| GTPγS | guanosine 5′-O-(3-[35S]thio)triphosphate |
| ICL | intracellular loop |
| NIH | National Cancer Institute |
| PBS | phosphate buffered saline |
| PDB | Protein Data Bank |
| RMSD | root-mean square deviations |
| TBS | Tris-buffered saline |
| TBST | TBS with Tween |
| TM | transmembrane domain |
| TMB | 3,3′,5,5′-tetramethylbenzidine |

and the co-crystallized orthosteric ligands MK-0812 and BMS-681 bind. The second is an allosteric binding pocket at the intracellular side of the receptor, for which evidence in chemokine receptors has been accumulating [14]. This is also backed by crystal structures of CCR7, CCR9 and CXCR2, all showing a spatially conserved intracellular allosteric binding site for small molecules [17–19]. Targeting this binding site with allosteric compounds, e.g. CCR2-RA-[*R*] [20] in CCR2, could prove beneficial as competition with chemokines is avoided.

It is estimated that approximately 20 % of cancers have mutations in GPCRs [21]. The Genomic Data Commons (GDC) from the National Cancer Institute (NIH) is one of the large-scale sequencing projects that collect cancer-associated mutations from patient biopsy material [22]. These mutations could alter receptor expression and function, which has previously been shown for other GPCRs, e.g. the adenosine $A_{2B}$ receptor and C-X-C chemokine receptor 4 [23,24]. However, cancer-related mutations might also alter the receptor's drugability.

In this research, cancer-related mutations were investigated for their effect on CCR2 activation, inhibition, and antagonist binding for both orthosteric and allosteric ligands. Mutations from the GDC database were narrowed down based on their location near binding sites or presence in conserved locations and motifs. One of the mutations resulted in loss of expression, while all affected the efficacy of receptor activation by CCL2 to various extents. An orthosteric and allosteric antagonist, INCB3344 and LUF7482, respectively, were chosen as prototypical antagonists to determine the effect of mutations on potential drug treatment. None of the selected mutants affected the potency for either antagonist significantly. Tritium labelled versions of these compounds were used to determine any change in affinity to the mutant receptors. Binding of the orthosteric radioligand [$^3$H]INCB3344 was significantly altered by four mutations, while two others inhibited binding of the allosteric radioligand [$^3$H]LUF7482 completely. This indicates that these CCR2 mutations might not be driver mutations, but our findings suggest that they may have impact on the efficacy of CCR2-targeting therapies and should therefore be considered in cancer drug discovery.

## 2. Materials and methods

### 2.1. Datamining and mutant selection

The X-ray resolved crystal structure of CCR2 isoform B (Protein Data Bank (PDB) identifier: 5T1A) was prepared with Free Maestro [25]: bond orders were assigned using the Cambridge Crystallographic Data (CCD) database, hydrogen atoms added and a single disulphide bond created between C113$^{3.25}$ and C190$^{45.50}$. Residues between N1002 and P1162 were removed since they correspond to the T4 lysozyme insert into intracellular loop 3 (ICL3). The S-(2-amino-2-oxoethyl)-L-cysteine 181 in ECL2 was mutated into cysteine and residues S226$^{5.62}$ to K240$^{6.32}$, corresponding to the sequence S226$^{5.62}$-RASKSRIPPPSREK-K240$^{6.32}$, originating from the M2 muscarinic acetylcholine receptor and used to ease crystallization, were reverted to the native sequence L226$^{5.62}$-KTLLRCRNEKKRH-R240$^{6.32}$. Residues C232$^{5.68}$ to E235 were then minimized in place to accommodate the newly created peptide bond linking R233 to R234 in ICL3. The system was then minimized using UCSF Chimera [26] through 100 steepest descent steps with step size 0.02 Å.

Residues were deemed in the vicinity of binding sites if any of their atoms lied within a radius of 5 Å of any atom of the co-crystalized BMS-681 and CCR2-RA-[*R*] ligands. This resulted in the identification of 36 residues around BMS-681 and 25 around CCR2–RA-[*R*].

Mutations in CCR2 were retrieved from the Genomic Data Commons (GDC) database, data release 22.0. Mutations were included if they corresponded with the aforementioned residues near one of the two binding sites. In addition, mutations located in conserved motifs were added to the selection [27].

### 2.2. Chemicals and reagents

The human recombinant chemokine CCL2 was purchased from PeproTech (Rocky Hill, NJ, USA). INCB3344, LUF7482 and CCR2-RA-[*R*] were synthesized in-house as described previously [28–30]. [$^3$H]INCB3344 (specific activity 26 Ci mmol$^{-1}$) was custom-labelled by Vitrax (Placentia, CA, USA) and [$^3$H]LUF7482 (specific activity 39.1 Ci mmol$^{-1}$) was custom-labelled by Roche (Basel, Switzerland). [$^{35}$S]GTPγS (guanosine 5′-O-(3-[$^{35}$S]thio)triphosphate), with a specific activity of 1250 Ci mmol$^{-1}$, was acquired from PerkinElmer (Waltham, MA, USA). Bovine serum albumin (BSA, fraction V) was purchased from Sigma (St. Louis, MO, USA). Bicinchoninic acid (BCA) and BCA protein assay reagent were purchased from Pierce Chemical Company (Rockford, IL, USA). HEK293T cells were obtained from ATCC (Manassas, VA, USA). All other chemicals and reagents were purchased from standard commercial sources.

### 2.3. Plasmid design and isolation

Primers were designed using the QuikChange® Primer Design feature (Agilent Technologies, CA, USA) and ordered via Integrated DNA Technologies (Coralville, IA, USA). A pcDNA3.1(+)-hCCR2b-wt plasmid with an N-terminal 3xhemagglutinin (HA) tag was used as a template for mutations. Mutations were generated with the QuikChange II Site-Directed Mutagenesis Kit (Agilent Technologies) according to the protocol. In short, 50 ng of the template was mixed with 10 μM forward and reverse primer, 1 μL of deoxyribonucleotide triphosphate (dNTP) mix, 2.5 μL of 10× reaction buffer and 2.5 U *PfuUltra* HF DNA polymerase in a total volume of 20 μL. The PCR reaction was performed in a T100™ Thermal Cycler (Biorad, CA, USA) for 22 cycles consisting of 30 s at 98 °C, 1 min at 55 °C and 10 min at 68 °C. The template DNA was then removed by incubating the mixture with 5 U of *Dpn I* restriction enzyme for 2 h at 37 °C before transforming the plasmids into XL-1 Blue supercompetent cells according to the kit's protocol. The plasmids were isolated with the QIAprep mini and midi plasmid purification kits (Qiagen, USA). Lastly, mutations were confirmed by double-strain DNA sequencing (LGTC, Leiden University, the Netherlands).

### 2.4. Cell culture, transfection and membrane preparation

HEK293T cells were grown in Dulbecco's Modified Eagle Medium

(DMEM) High Glucose, supplemented with 10 % fetal calf serum, 2 mM glutamine 100 IU/mL penicillin, and 100 μg/mL streptomycin under a humidified atmosphere with 5 % $CO_2$, at 37 °C. Cells were subcultured twice weekly by trypsinization. Cells between passage 3 and 15 were transfected with 5 μg plasmid DNA using polyethyleneimine in a 1:6 ratio. Sodium butyrate (5 mM) was added after 24 h, and cells were used for either ELISA or membrane preparation after an additional 24 h in culture. For membrane preparation, cells were scraped into phosphate buffered saline (PBS) and centrifuged for 5 min at 3000 rpm. The pellet was then resuspended in ice-cold buffer of 50 mM Tris-HCl, pH 7.4, supplemented with 5 mM $MgCl_2$ before homogenization with an Ultra Turrax homogenizer (IKA-Werke GmbH & Co. KG, Staufen, Germany). In two centrifugation steps using an Optima LE-80 K ultracentrifuge (Beckman Coulter, Inc., Fullerton, CA) at 31000 rpm for 20 min at 4 °C, the membrane fraction was separated. The resulting pellet was resuspended in ice-cold buffer of 50 mM Tris-HCl (pH 7.4), supplemented with 5 mM $MgCl_2$ and stored at −80 °C. Protein concentrations of membranes were determined using the BCA protein determination protocol [31].

### 2.5. ELISA

HEK293T cells were transfected as described in section 2.3. 24 h after transfection, cells were washed with PBS and detached with PBS/EDTA and resuspended in culture medium supplemented with 5 mM sodium butyrate. They were plated out to $1 \times 10^5$ cells per well in poly-D-lysine pre-treated, tissue culture treated, flat-bottom 96 wells plates and kept under a humidified atmosphere with 5 % $CO_2$, at 37 °C. After 24 h, the cells were washed with PBS and fixed with 4 % formaldehyde for 10 min at RT. After washing twice with Tris-buffered saline (TBS), the cells were treated with blocking buffer (2 % (w/v) BSA in TBS with Tween (TBST)) for 1 h at RT while shaking. Wells were washed with TBST and afterwards the primary antibody RabbitαHA was added at a dilution of 1:2500 in assay buffer (0.1 % (w/v) BSA in TBST). After 1 hr at RT while shaking, cells were washed three times with TBST. The secondary HRP-conjugated GoatαRabbit antibody at a dilution of 1:2500 in assay buffer was subsequently added for 30 min at RT while shaking. After a final three time washing with TBS, 3,3′,5,5′-tetramethylbenzidine (TMB) was added and incubated in the dark for ~ 5 min at RT before stopping the reaction with 1 M of $H_3PO_4$ solution. Hereafter, the absorbance was read at 450 nm after 5 min at RT using the EnVision multilabel plate reader (PerkinElmer, Inc, Waltham, MA, USA).

### 2.6. [$^{35}$S]GTPγS binding assay

[$^{35}$S]GTPγS binding assays were performed as previously described. [30] In short, assays were performed in a total volume of 100 μL containing assay buffer (50 mM TRIS-HCl (pH 7.4), 50 mM MgCl2, 100 mM NaCl, 1 mM EDTA, 0.05 % (w/v) BSA), 0.5 mg/mL saponin, 10 μM GDP and 20 μg of membranes. Membranes were incubated with increasing concentrations of CCL2 to determine $EC_{50}$ and $EC_{80}$ values. Membranes were incubated with increasing concentrations of INCB3344 or LUF7482 and an $EC_{80}$ concentration of CCL2 to determine the antagonist $IC_{50}$ values. Basal activity was determined in the absence of CCL2 or antagonists. The reagent mixture was incubated for 30 min at 25 °C before addition of 0.3 nM [$^{35}$S]GTPγS followed by 90 min at 25 °C while shaking, before removing unbound radioligand with ice-cold washing buffer (50 mM TRIS-HCl (pH 7.4), 5 mM $MgCl_2$) on GF-C filters using a PerkinElmer Filtermate harvester (PerkinElmer, Groningen, The Netherlands). Radioactivity was measured through scintillation spectrometry using the P-E 2450 Microbeta$^2$ scintillation plate counter (PerkinElmer, Groningen, The Netherlands) after the addition of 25 μL Microscint scintillation cocktail (PerkinElmer, Groningen, The Netherlands).

### 2.7. [$^3$H]INCB3344 and [$^3$H]LUF7482 homologous displacement assay

Homologous displacement assays for both [$^3$H]INCB3344 and [$^3$H]LUF7482 were performed similarly in a total reaction volume of 100 μL containing 50 mM TRIS-HCl (pH 7.4), 5 mM $MgCl_2$, 0,1 % CHAPS, 5–40 μg membranes, ~1.5, ~5 and ~ 9.5 nM for [$^3$H]INCB3344 and ~ 1, ~3 and ~ 9 nM for [$^3$H]LUF7482. Total binding was determined by addition of the vehicle only, while non-specific binding was determined by addition of 10 μM INCB3344 or CCR2-RA-[*R*]. Note, DMSO concentrations were kept constant at 1 % (v/v). For both radioligands, reaction mixtures were incubated for 2 h at 25 °C while shaking before harvesting as explained in section 2.5.

### 2.8. Docking of INCB3344 and LUF7482 and in silico mutagenesis

The previously prepared crystal structure of CCR2 isoform B in section 2.1 (Protein Data Bank identifier: 5T1A) was prepared for docking with ICM Pro, v3.9-1b (Molsoft LLC, San Diego, CA) [32,33]: water molecules were removed; hydrogen atoms were added and their position optimized along the orientation and protonation states of histidine and cysteine residues, the orientation of glutamine and asparagine residues and the tautomeric state of ligands. The molecular structures of BMS-681 and INCB3344 were sketched with ICM and docked within the region defined by residues in the vicinity of the co-crystalized orthosteric ligand as defined by ICM Pro. Default thoroughness (3), and number generated conformations (3), and enhanced Born scoring were used. Similarly, the structures of CCR2-RA-*[R]* and LUF7482 were sketched and docked in the region defined by residues in the vicinity of the co-crystalized allosteric ligand.

Amino acids of interest were mutated with Free Maestro using the structure of CCR2 isoform B with docked INCB3344 and LUF7482 along with co-crystalized BMS-681 and CCR2-RA-*[R]*. The disruption or establishment of interactions deriving from these mutations were identified along with the change in size and electrostatic distribution.

### 2.9. Data analysis and statistics

Data was analysed using GraphPad Prism 9.0 (GraphPad software, San Diego, CA, USA). [$^{35}$S]GTPγS activation or inhibition assays were analysed using the non-linear regression function “log (agonist or inhibitor) vs. response (three parameters)” to obtain $EC_{50}$, $IC_{50}$ and $E_{max}$ values. Homologous displacement experiments were analysed using the “One site – Homologous” function to obtain $K_D$ and $B_{max}$ values. Ordinary one-way ANOVA tests were performed for all data sets to compare mutant values to WT receptor values. Data is shown as means of at least three separate experiments performed in duplicate. Observed differences were considered statistically significant if p-values were below 0.05.

## 3. Results

### 3.1. Selection of cancer-related CCR2 mutants

Mutations found in patient solid tumours were retrieved from the GDC portal, resulting in 125 mutations for CCR2 of which 75 were missense mutations (Fig. 1A). These were further narrowed down using a 5 Å spherical range around the co-crystallized ligands BMS-681 and CCR2-RA-[*R*] in the crystal structure of CCR2 (Fig. 1B). The resulting 5 orthosteric and 2 allosteric binding site mutations were supplemented with 4 mutations found in conserved motifs or conserved residues (Fig. 1C). A final list of 10 CCR2 mutations was obtained, as one of the mutants fitted in either category. Of these, S101P$^{2.63}$, E105Q$^{23.49}$, V107A$^{23.51}$, F116V$^{3.28}$ and F116Y$^{3.28}$ are located near the orthosteric binding site. V107A$^{23.51}$ and F116V$^{3.28}$ are located in extracellular loop 1 (ECL1), while S101P$^{2.63}$, F116V$^{3.28}$ and F116Y$^{3.28}$ are located in either transmembrane domain 1 (TM1) or 2 (TM2). L134Q$^{3.46}$ and D137N$^{3.49}$

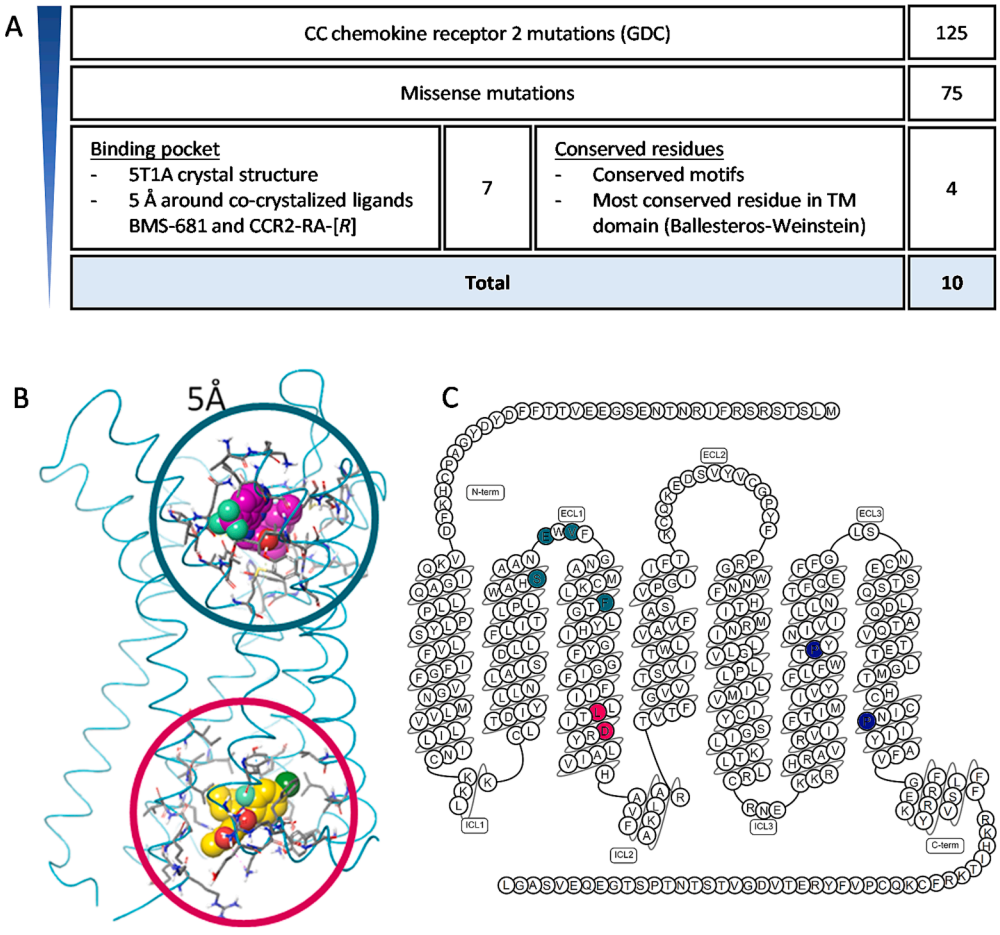


**Fig. 1. Selection cancer-related mutants.** (A) Flow-chart showing how mutations were obtained and narrowed down from the GDC database. (B) CCR2 homology model of 5T1A bound to BMS-681 (purple spheres) and CCR2-RA-[*R*] (yellow spheres), showing amino acids located near either orthosteric (green circle) or allosteric (magenta circle) binding site. (C) Snake-plot highlighting selected residues, i.e. orthosteric binding pocket (green), near the allosteric binding pocket (magenta) or conserved residues (blue). (For interpretation of the references to colour in this figure legend, the reader is referred to the web version of this article.)

are located near the intracellular allosteric binding site in TM3, where the latter is also part of the DRY motif [34]. P258L$^{6.50}$ is located in the xWxP motif, and P302L$^{7.50}$ and P302R$^{7.50}$ in the NPxxY motif in TM6 and TM7, respectively.

### 3.2. Expression and function of CCR2 mutants

HEK293T cells, which do not endogenously express the receptor, were transfected with WT or mutant HA-CCR2 DNA and their expression on the cell surface was confirmed using an ELISA (Fig. 2A). Expression is shown as fold over mock, with mock cells being transfected with an empty pcDNA3.1 plasmid. F116V$^{3.28}$, F116Y$^{3.28}$, D137N$^{3.49}$, P302L$^{7.50}$ and P302R$^{7.50}$ were expressed to a similar or higher extent as WT. S101P$^{2.63}$, E105Q$^{23.49}$, V107A$^{23.51}$ and L134Q$^{3.46}$ showed a markedly lower expression, with folds over mock ranging between 1.3 and 2-fold. P258L$^{6.50}$ was the only mutant that appears not to be expressed on the cell surface. However, since it was possible this mutant is inefficiently trafficked and still expressed on other intracellular membranes, it was taken along for further experiments.

Receptor function of the mutant receptors was determined using [$^{35}$S]GTPγS binding assays that detect G protein activation in response to increasing concentrations of the main cognate ligand CCL2 (Fig. 2B, 2C and 2D, Table 1). A number of mutants was not be activated at all, namely S101P$^{2.63}$, P258L$^{6.50}$, P302R$^{7.50}$ and P302L$^{7.50}$, of which S101P$^{2.63}$ and P258L$^{6.50}$ showed low or no expression as determined by ELISA, respectively (Fig. 2A). The six other mutants showed a significantly decreased $E_{max}$ compared to WT, in a range of 22–65 %. Specifically, only V107A$^{23.51}$ and F116Y$^{3.28}$ showed over 50 % activation. Interestingly, these six mutations had no effect on CCL2 potency or basal receptor activation (Fig. 2, Table 1).

### 3.3. Inhibition of mutant CCR2

Inhibition of WT and mutant CCR2 by the orthosteric antagonist INCB3344 and allosteric antagonist LUF7482 was determined for all mutant receptors that showed activation (Fig. 3A and 3B). A submaximal concentration of CCL2 was used to determine the potency of these prototypical antagonists at each mutants (Fig. 3C and 3D, Table 1). Overall, INCB3344 was more potent in inhibiting CCL2-induced G protein activation than LUF7482 (Fig. 3, Table 1). Of note, potencies could not be accurately determined for E105Q$^{23.49}$, F116V$^{3.28}$, L134Q$^{3.46}$ and D137N$^{3.49}$ due to a too small level of activation as illustrated by large standard deviations of approximately one log unit. For the remaining mutants V107A$^{23.51}$ and F116Y$^{3.28}$, no significant differences in potency were found for either antagonist (Fig. 3, Table 1).

### 3.4. Homologous displacement at mutant CCR2

Initial binding experiments showed that [$^{3}$H]INCB3344 could still bind E105Q$^{23.49}$, V107A$^{23.51}$, F116V$^{3.28}$, F116Y$^{3.28}$, L134Q$^{3.46}$ and D137N$^{3.49}$ (Fig. 4A). However, no binding was detected for S101P$^{2.63}$, P258L$^{6.50}$, P302R$^{7.50}$ and P302L$^{7.50}$ using this orthosteric radioligand (Fig. 4B). Not surprisingly for S101P$^{2.63}$, P258L$^{6.50}$ which showed low or no expression as show in Fig. 2A. Interestingly, these same mutations also showed no window for [$^{3}$H]LUF7482 binding. However, [$^{3}$H]LUF7482 could also not bind L134Q$^{3.46}$ and D137N$^{3.49}$ unlike [$^{3}$H]INCB3344. A significant window for [3H]LUF7482 was only observed for E105Q$^{23.49}$, V107A$^{23.51}$, F116V$^{3.28}$, F116Y$^{3.28}$, next to WT.

As the potencies of INCB3344 and LUF7482 were difficult to determine in [$^{35}$S]GTPγS assays for some mutants, homologous displacements were performed with the tritium labelled versions of these

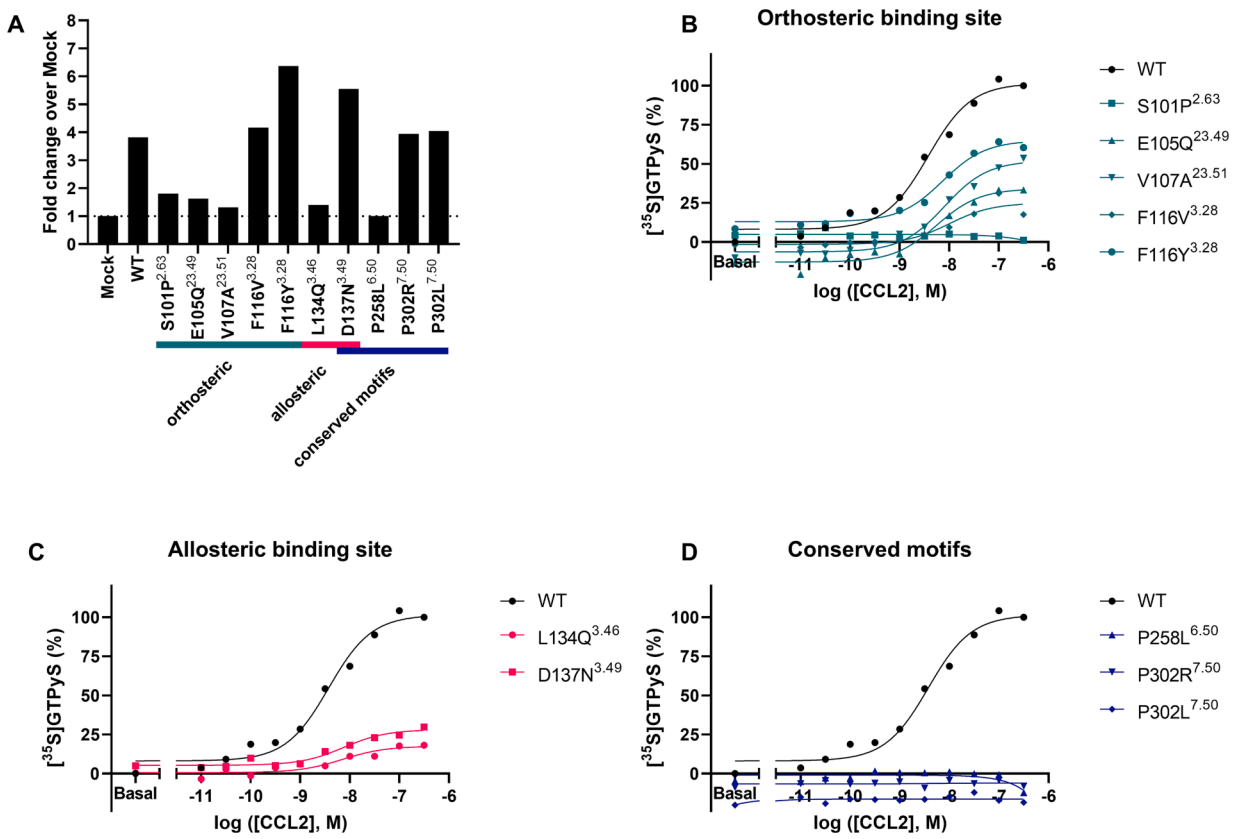


**Fig. 2. Receptor expression and activation** (A) Receptor expression of (mutant) HA-CCR2 transiently transfected into HEK293T cells. Mock cells are transfected with the empty vector. Data is represented as fold over mock of a representative experiment of at least two separate experiments performed in duplicate. (B, C and D) G protein activation of (mutant) CCR2 with mutations located in orthosteric (green), allosteric (magenta) or conserved residues (blue). The activation of the WT at 316 nM CCL2 was set as 100 %, whereas. 0 % basal of WT was set at 0 %. Data is shown as a representative graph of at least three separate experiments performed in duplicate. (For interpretation of the references to colour in this figure legend, the reader is referred to the web version of this article.)

**Table 1**
G protein activation and inhibition of WT and mutant CCR2 performed with membranes of HEK293T cells transfected with cancer-associated CCR2 mutants.

| | $pEC_{50}$ ($EC_{50}$, nM) | Basal (Fold over WT)[a] | $E_{max}$ (%) | $pIC_{50}$ ($IC_{50}$, nM) INCB3344 | $pIC_{50}$ ($IC_{50}$, nM) LUF7482 |
|---|---|---|---|---|---|
| **WT** | 8.3 ± 0.2 (4.9) | 1 | 101 ± 2 | 7.8 ± 0.3 (21) | 6.9 ± 0.1 (141) |
| **E105Q$^{23.49}$** | 8.4 ± 0.2 (4.4) | 0.9 ± 0.1 | 37 ± 12**** | 7.1 ± 1.2 (182) | 6.6 ± 0.2 (262) |
| **V107A$^{23.51}$** | 8.1 ± 0.1 (7.7) | 0.8 ± 0.0 | 53 ± 12**** | 8.1 ± 0.3 (10) | 6.8 ± 0.0 (165) |
| **F116V$^{3.28}$** | 8.1 ± 0.1 (8.8) | 0.9 ± 0.1 | 25 ± 7**** | 6.9 ± 1.0 (323) | 7.3 ± 0.3 (55) |
| **F116Y$^{3.28}$** | 8.3 ± 0.2 (5.7) | 1.0 ± 0.0 | 65 ± 10**** | 7.9 ± 0.1 (12) | 6.9 ± 0.2 (151) |
| **L134Q$^{3.46}$** | 8.5 ± 0.3 (2.1) | 1.1 ± 0.2 | 21 ± 4**** | 7.4 ± 1.0 (153) | 6.3 ± 0.3 (633) |
| **D137N$^{3.49}$** | 8.4 ± 0.2 (4.8) | 1.1 ± 0.0 | 29 ± 3**** | 8.3 ± 0.7 (11) | 5.7 ± 1.2 (13 306)* |

Values are represented as mean ± SD of at least 3 separate experiments performed in duplicate. Basal, $pEC_{50}$ and $E_{max}$ or maximal activation at 316 nM were determined [$^{35}$S]GTPyS assays in response to increasing concentrations of CCL2 on transiently transfected U2OS membranes. Inhibition by INCB3344 and LUF7482 were determined by inhibiting an $EC_{80}$ concentration of CCL2. Mutants S101P$^{2.63}$, P256L$^{6.50}$, P302R$^{7.50}$ and P302L$^{7.50}$ showed no activation, so no potency of CCL2 or either antagonist could be determined. * $P < 0.05$, **** $P < 0.0001$. Significance was determined using a one-way ANOVA compared to WT.
[a]Fold over WT was determined compared to WT within experiments.

compounds (See Fig. 4C and 4D for representative graphs). In addition to the potency, the total concentration of receptors was determined ($B_{max}$) in these experiments. Note that the ELISA assays measure the presence of the HA-tag of the receptor, but do not give information on the receptor itself. The $B_{max}$ determinations followed a similar trend between radioligands (Table 2). However, receptor expression levels seemed consistently higher when [$^3$H]LUF7482 was used instead of [$^3$H]INCB3344. F116V$^{3.28}$ (8.13 ± 0.62 and 11.34 ± 4.49 pmol/mg) was the only mutant which showed significantly higher expression than WT (6.42 ± 0.54 and 9.81 ± 0.26 pmol/mg), for [$^3$H]INCB3344 and [$^3$H]LUF7482 respectively. E105Q$^{23.49}$, V107A$^{23.51}$ and F116Y$^{3.28}$ all showed lower 1.5 to 2-fold difference in expression compared to WT for either radioligand. L134Q$^{3.46}$ and D137N$^{3.49}$ were the lowest (detectable) expressing mutants, with a $B_{max}$ of 0.57 ± 0.07 and 1.95 ± 0.62 pmol/mg protein for [$^3$H]INCB3344, respectively. These mutants were not detected using [$^3$H]LUF7482.

The affinity of [$^3$H]INCB3344 was significantly but marginally affected by mutations L134Q$^{3.46}$ (8.9 ± 0.09) and D137N$^{3.49}$ (8.6 ± 0.05) compared to WT (8.7 ± 0.08) (Table 2). Only F116V$^{3.28}$ and F116Y$^{3.28}$ altered [$^3$H]INCB3344′s affinity somewhat more, with $K_D$ values of 7.5 ± 0.02 and 8.5 ± 0.08, respectively, with a compelling ten-fold difference between them. With the exception of the loss of binding of mutants L134Q$^{3.46}$ and D137$^{N3.49}$, affinity for [$^3$H]LUF7482 was not altered significantly in comparison to WT (Table 2).

### 3.5. Computational calculations for loss of binding mutants

The redocking of BMS-681 and CCR2-RA-[*R*] in their respective binding sites resulted in binding poses almost identical to that of crystals

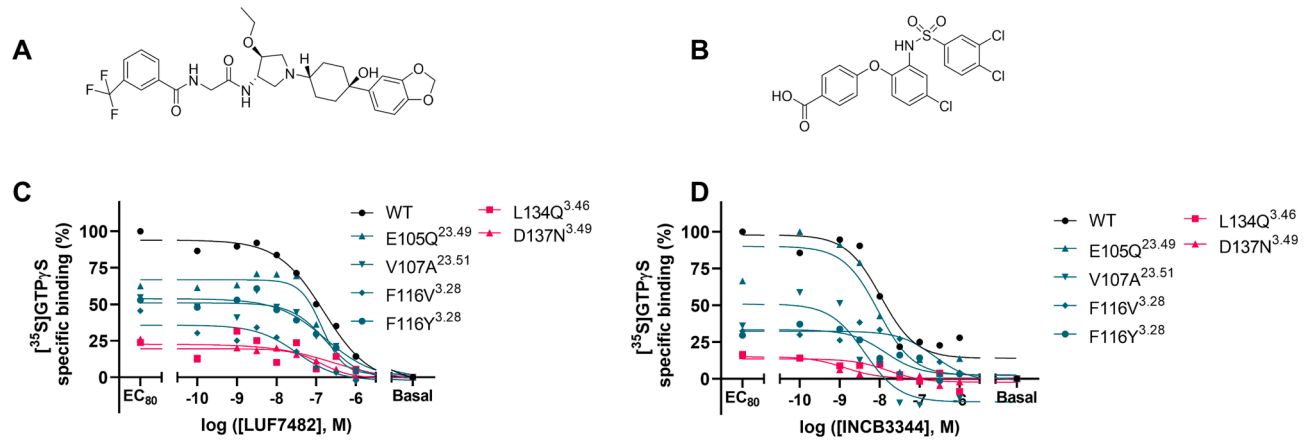


**Fig. 3. Receptor inhibition of CCL2-induced G protein activation** Chemical structures of (A) orthosteric antagonist INCB3344 and (B) allosteric antagonist LUF7482. (C and D) Inhibition of WT and mutant CCR2 by INCB3344 or LUF7482 on transiently transfected U2OS membranes in the presence of an $EC_{80}$ concentration of CCL2. For WT and each mutants, basal was set to 0 % while the $EC_{80}$ activation of WT was set to 100 % in all cases. Data is shown as a representative graph of at least three separate experiments performed in duplicate.

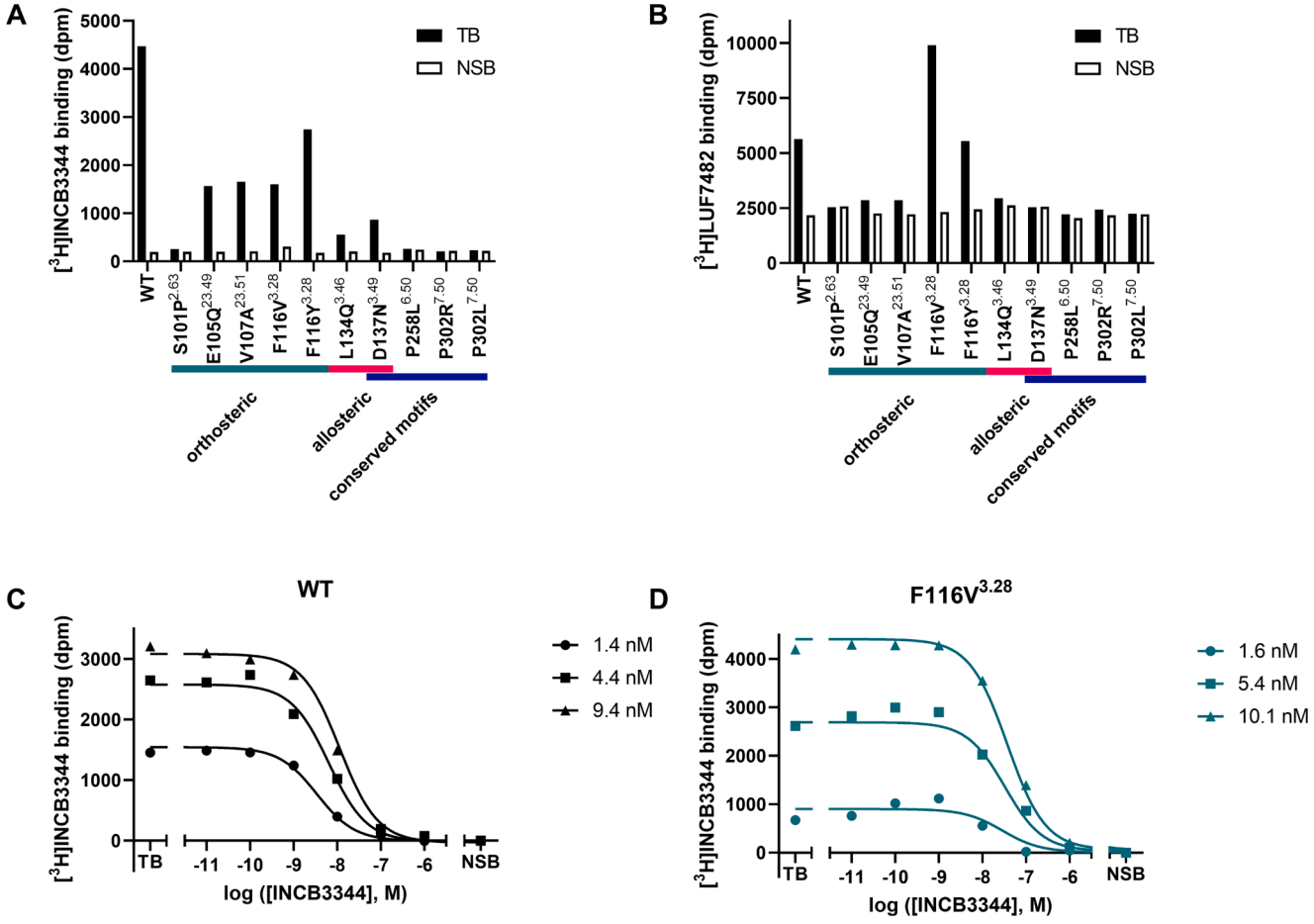


**Fig. 4. Radioligand binding experiments with the orthosteric radioligand [$^3$H] INCB3344 and allosteric radioligand [$^3$H] LUF7482.** (A and B) Single point binding of [$^3$H]INCB3344 and [$^3$H]LUF7482 at (0.8 mg/mL protein). Data shown are total binding (TB) and non-specific binding (NSB) of a representative experiment of at least two experiments performed in duplicate. (C and D) Homologous displacement curves of WT and F116V CCR2 for [$^3$H]INCB3344. Data shown are representative curves of at least three experiments shown in duplicate.

with root-mean square deviations (RMSD) of atomic coordinates of 0.42 Å and 0.58 Å and docking scores of –33.59 and –23.78 for BMS-681 and CCR2-RA-[*R*] respectively. Although the docking score of CCR2-RA-[*R*] was higher than the reference score of –32.0, the low RMSD proved the capacity of the employed docking algorithm to recover the binding poses almost coinciding with their position in the crystal structures.

Substructures of the docked INCB3344, with docking score of −29.84, and co-crystalized BMS-681 (data not shown) overlapped significantly well with a RMSD of 0.81 Å with conserved hydrogen bonds with $Y49^{1.39}$, $Q288^{7.36}$ and $T292^{7.40}$ and hydrophobic

**Table 2**
Homologous displacement of ~ 1.5, ~5 and ~ 9.5 nM [$^3$H]INCB3344 and ~ 1, ~3 and ~ 9 nM [$^3$H]LUF7482 performed with membranes of HEK293T cells transfected with cancer-associated CCR2 mutants.

| | [$^3$H] INCB3344 | | [$^3$H] LUF7482 | |
|---|---|---|---|---|
| | $B_{max}$ (pmol/mg) | $pK_D$ ($K_D$, nM) | $B_{max}$ (pmol/mg) | $pK_D$ ($K_D$, nM) |
| **WT** | 6.42 ± 0.54 | 8.7 ± 0.08 (1.8) | 9.81 ± 0.26 | 8.2 ± 0.03 (6.5) |
| **E105Q$^{23.49}$** | 3.99 ± 0.18*** | 8.8 ± 0.05 (1.4) | 5.55 ± 1.51 | 8.2 ± 0.07 (6.3) |
| **V107A$^{23.51}$** | 3.71 ± 0.29**** | 8.8 ± 0.06 (1.7) | 4.56 ± 0.84* | 8.1 ± 0.1 (8.6) |
| **F116V$^{3.28}$** | 8.13 ± 0.62** | 7.5 ± 0.02**** (30) | 11.34 ± 4.49 | 8.0 ± 0.1 (11) |
| **F116Y$^{3.28}$** | 5.11 ± 0.69* | 8.5 ± 0.08*** (3.3) | 4.23 ± 1.22* | 8.1 ± 0.3 (8.8) |
| **L134Q$^{3.46}$** | 0.57 ± 0.07**** | 8.9 ± 0.09* (1.2) | ND | ND |
| **D137N$^{3.49}$** | 1.95 ± 0.62**** | 8.6 ± 0.05* (2.6) | ND | ND |

Values are represented as mean ± SD of three separate experiments performed in duplicate. ND, not determined due to no or low radioligand binding. Mutants S101P$^{2.63}$, P256L$^{6.50}$, P302R$^{7.50}$ and P302L$^{7.50}$ showed no or low radioligand binding, so $B_{max}$ and $pK_D$ values could not be determined * $p < 0.05$, ** $p < 0.01$, *** $p < 0.005$, **** $P < 0.0001$. Significance was determine using a one-way ANOVA compared to WT.

interactions with L44$^{1.34}$ and V289$^{7.37}$.

The docked pose of LUF7482, with a docking score of –23.56, showed conserved interactions with the backbone of F310$^{8.48}$ and hydrophobic interactions with I66$^{1.56}$, L97$^{2.59}$ and I245$^{6.37}$ (data not shown). Additionally, the π-stacking interaction with Y305$^{7.53}$ was conserved and a π-cation interaction as well as two electrostatic interactions between the docked pose of the benzoic acid moiety of LUF7482 and R138$^{3.40}$, K71$^{12.48}$ and K311$^{8.49}$ were obtained.

Considering these docked poses of INCB3344 and LUF7482, the impact of mutated residues on their respective binding sites was evaluated by *in silico* mutagenesis. Although all mutations have gone through this protocol, three examples will be discussed. These include the mutants with the largest impact on either discussed binding site, as well as an example of the considerable effect of a proline mutation.

With regards to the orthosteric binding site, the mutation of F116$^{3.28}$ into valine disrupts the π-stacking interaction formed with W98$^{2.60}$ (Fig. 5A). The latter amino acid is stabilized via a hydrogen bond between the nitrogen of its indole and the hydroxyl of the side-chain of T94$^{2.56}$, after its fused benzene ring is able to rotate into the binding site therefore introducing steric hindrance. The mutation to tyrosine reinstates this π-stacking interaction but introduces a polar hydroxyl group on the hydrophobic interface formed by T94$^{2.56}$, L97$^{2.59}$, M112$^{3.24}$ and L119$^{3.31}$ between TM2 and TM3.

The allosteric residue D137$^{3.49}$ was mutated to an asparagine which resulted in a loss of electrostatic interaction with R138$^{3.50}$ (Fig. 5B). This allowed R138$^{3.50}$ to freely expand towards the allosteric binding site, possible disrupting LUF7482 binding.

Mutations involving proline, S101P$^{2.63}$, P258L$^{6.50}$, P302R$^{7.50}$ and P302L$^{7.50}$, introduced major structural changes. P258$^{6.50}$ is responsible for the bend in TM6 and its mutation to leucine, in spite of keeping the local hydrophobicity, allowed for the restoration of the *i* to *i* + *3* backbone interaction with L254$^{6.46}$ and straightens TM6 (Fig. 5C). A loss of a proline, as for P258L$^{6.50}$, P302R$^{7.50}$ and P302L$^{7.50}$, or a gain of a proline, as for S101P$^{2.63}$, could therefore severely interrupt helix conformation and thereby protein conformation.

## 4. Discussion and conclusion

Cancer is one of the leading causes of death worldwide, with GPCRs affecting all aspects of the disease [2]. GPCRs have found to be mutated in approximately 20 % of cancers, which can affect receptor pharmacology [21]. Here, cancer-related mutations in CCR2, a receptor highly involved in immunosuppression and cancer metastasis, were explored. Mutations were extracted from the GDC database, v22.0, which resulted in a list of 125 mutations of which 75 were missense. This was further narrowed down by cross-referencing with residues within 5 Å of co-crystallized ligands in the CCR2 crystal structure (PDB: 5T1A) and conserved residues. This resulted in a list of 10 mutations that were investigated for receptor expression, function and effect on orthosteric and allosteric antagonist inhibition and binding.

All mutants were transiently transfected into HEK293T cells. Overall, receptors with either a mutation to or from a proline showed no expression (P258L$^{6.50}$) or were detrimental for receptor function (S101P$^{2.63}$, P302L$^{7.50}$ and P302R$^{7.50}$) (Fig. 2). This was confirmed by *in silico* mutagenesis (Fig. 5), which showed that these proline mutations disturbed the structure of the respective alpha-helices involved, leading to issues with CCR2 architecture, and subsequently expression and/or activation. Highly conserved prolines such as those located at 6.50 and 7.50 in the conserved motifs xWxP and NPxxY respectively, induce a kink in the TM helices and are critical for a see-saw movement of the helix during receptor activation [35]. Therefore, it is not surprising that P302L$^{7.50}$ and P302R$^{7.50}$ mutants showed a loss of receptor activation, as the receptor is no longer able to complete this movement. Noteworthy is that mutations in highly conserved positions of TM regions, including 6.50 and 7.50, rank among the most frequent in the GDC and 1000 genomes datasets, as shown recently by Bongers *et al.* [36].

All mutants that could be activated showed a decreased efficacy but no change in potency in response to CCL2 (Fig. 2, Table 1). Homologous displacement assays showed lower receptor expression compared to WT for most of the tested mutants. For example E105Q$^{23.49}$ and V107A$^{23.51}$ located in ECL1 showed an approximate two-fold decrease in expression, as measured with two different radioligands (Table 2). *In silico* mutagenesis demonstrated no direct consequences in receptor conformation (data not shown) and ECL1 has been shown not to be involved in chemokine recognition in a recent cryoEM structure of a CCL2-CCR2-G-protein complex [37]. Hence, the reduced activation is likely related to a decreased receptor expression. Of the mutants, F116Y$^{3.28}$ showed the highest efficacy in response to CCL2, while F116V$^{3.28}$ only showed an $E_{max}$ of 25 ± 7 % compared to WT, even though it had an increased receptor expression (Fig. 4, Table 2). *In silico* mutagenesis indicated π-stacking between F116 and T94 that was retained for the F116Y$^{3.28}$ mutant but lost for F116V$^{3.28}$, causing a disruption in the orthosteric binding pocket. In the recent cryo-EM structure of the active CCR2 conformation, extensive hydrogen bonding in this area with a direct interaction of the N-terminus of CCL2 to the neighbouring residue T117$^{3.29}$ was shown [37]. The reduction in F116V$^{3.28}$ activation thus appears to be binary: 1) consisting of a collapse of the orthosteric binding pocket and 2) subsequent reduced interaction with the chemokine N-terminal tail.

The mutation of D137$^{3.49}$ is located near the allosteric binding pocket, and is part of the DRY motif [38]. This aspartic acid forms an ionic lock with R$^{3.50}$, stabilizing the inactive state of the receptor [15]. Mutation of the aspartic acid in the DRY motif has been proposed to lead to constitutively active mutants (CAMs) in rhodopsin-like receptors, as it was suggested that the equilibrium between deprotonation and protonation of aspartic acid is involved in receptor activation [39–41]. This has been validated for a number of class A GPCRs, as reviewed by Rovati *et al.* [42], but chemokine receptors have generally been found to be constitutively inactive mutants (CIMs). These include CCR3 [43], CCR5 [44,45] and CXCR1 [46]. In this research, none of the mutants, including D137N$^{3.49}$, could be classified as a CAM as there was no increased basal activity observed. D137N$^{3.49}$ is best classified as a CIM, as the maximal activation of this mutant reached 21 ± 4 % compared to WT (Fig. 2C and Table 1). Mutants S101P$^{2.63}$, P302R$^{7.50}$ and P302L$^{7.50}$ are to be classified as loss of function mutants, since even high

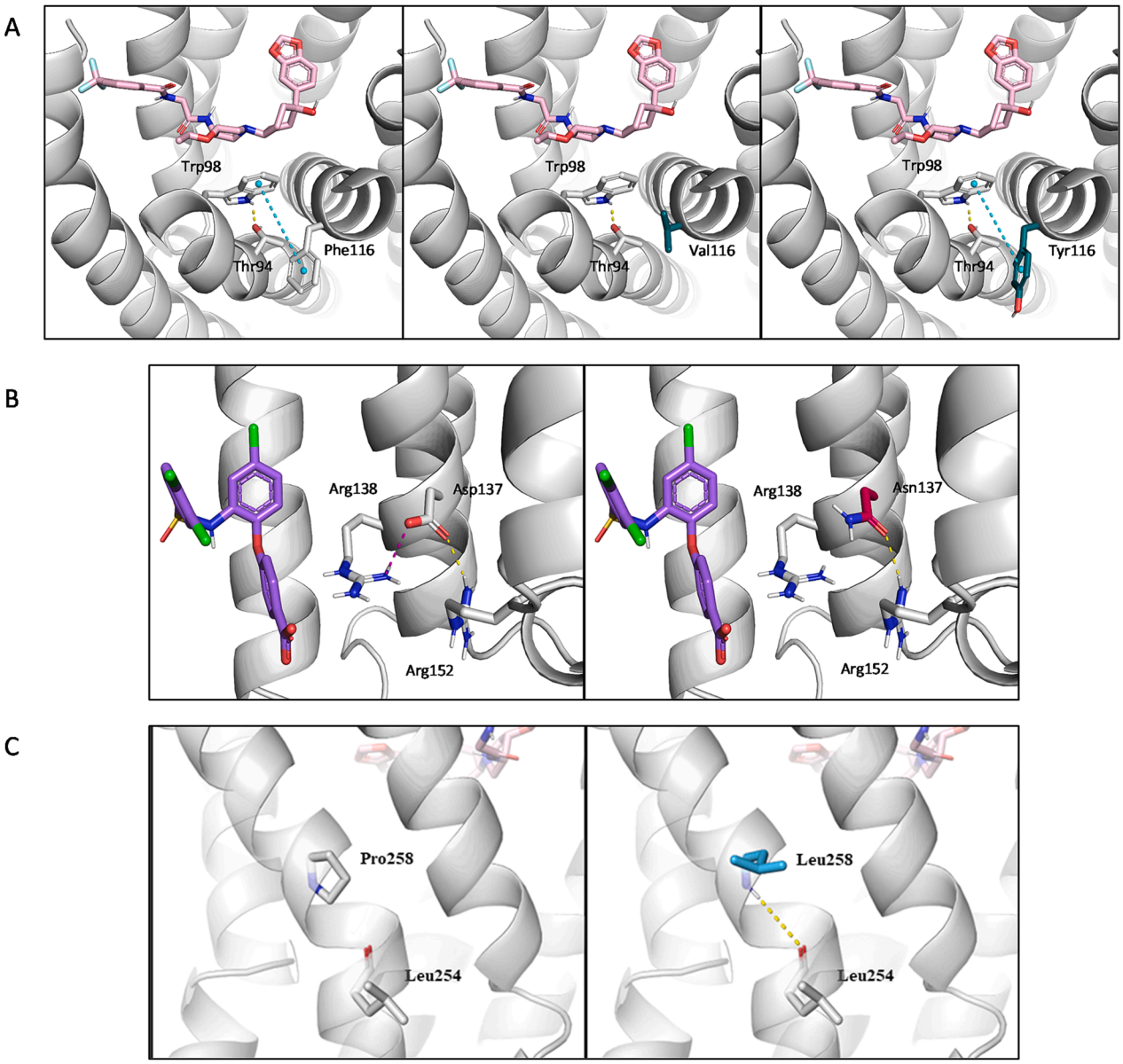


**Fig. 5. Interaction patterns of CCR2 with INCB3344 and LUF7482** (A) View of orthosteric binding site of WT receptor (left, grey sticks and ribbons) with INCB3344 (pink sticks). π-stacking interaction (blue dashes) between Thr94 and Phe116 with loss of interaction for mutant F116V$^{3.28}$ (middle, green sticks) and preserved interaction for mutant F116Y$^{3.28}$ (right, green sticks). (B) View of allosteric binding site of WT receptor (left) with LUF7482 (purple sticks). Electrostatic interaction (purple dashes) between Arg138 and Asp137 is lost for mutant D137N$^{3.46}$ (right, magenta sticks). (C) View of WT receptor (left) and the gained hydrogen bond (yellow dashes) for mutant P258L$^{6.50}$ (right, blue sticks). (For interpretation of the references to colour in this figure legend, the reader is referred to the web version of this article.)

concentrations of CCL2 did not activate these receptors (Fig. 2B, 2D and Table 1).

In addition to functional characterization of CCR2, two antagonists targeting either the orthosteric or allosteric binding site were studied as proxies for their respective drug classes (Figs. 3 and 4, Table 1 and 2). Currently, most antagonists target the orthosteric binding site of CCR2, but the intracellular allosteric binding site is gaining interest due to selectivity and insurmountability of the compounds' inhibitory action [14]. Moreover, CCR2 is gaining interest as an anti-cancer target due to its involvement in immunosuppression and metastasis formation [6]. Hence, multiple cancer-focussed clinical trials are ongoing at the time of writing to inhibit CCR2 in cancer, such as the orthosterically binding BMS-813160 (NCT03184870, NCT04123379) and CCX872 (NCT02345408), of which the structure is yet unknown. In this study, we found no significant differences between mutants and WT in inhibition of G protein activation in [$^{35}$S]GTPγS assays (Fig. 3 and Table 1). However, not all of the mutant receptors could be accurately analysed in this assay. On the other hand, the binding experiments did reveal clear differences (Fig. 4 and Table 2). F116V$^{3.28}$ and to a lesser extent F116Y$^{3.28}$, showed a reduced affinity for the orthosteric antagonist [$^{3}$H]INCB3344. As mentioned before, the π-stacking between T94 and F116 is important for structural integrity of the orthosteric binding pocket according to *in silico* mutagenesis. This interaction is retained for F116Y$^{3.28}$, but not for F116V$^{3.28}$. For the latter, T94 is able to move freely in the binding pocket, possibly interrupting orthosteric antagonist binding and thus explaining the decrease in its affinity.

[$^{3}$H]LUF7482 binding was completely lost for allosteric mutants L134Q$^{3.46}$ and D137N$^{3.49}$. *In silico* mutagenesis showed electrostatic interactions between D137$^{3.49}$ and R138$^{3.50}$ (Fig. 5B), where interruption of this interaction caused by D137N$^{3.49}$ caused R138 to move freely

within the allosteric binding pocket thereby displacing LUF7482. Interestingly, [$^3$H]INCB3344 binding was also significantly altered by L134Q$^{3.46}$ and D137N$^{3.49}$. Binding cooperativity has been reported in work describing a CCR2 X-ray structure in complex with both an orthosteric and allosteric antagonist, i.e. protein (thermos-)stability was synergistically increased by binding of both an orthosteric and allosteric antagonist [15]. This synergy has also been reported by Zweemer *et al.* for CCR2, where orthosteric antagonists increased allosteric antagonist binding and *vice versa* [47]. In addition, they detected a significant increase in potency for the orthosteric antagonist in the V244A$^{6.36}$ mutation located in the allosteric binding site, whereas the allosteric antagonist could no longer bind [48]. This demonstrates that mutations can not only affect the receptor and ligand binding locally, but also indirectly by changing the state of the receptor.

As GPCRs are highly mutated in cancer [21], loss of antagonist efficacy or even ineffectiveness of CCR2 as a drug target should be considered. Only a fraction of cancer-related mutant GPCRs in the GDC database have been studied. Furthermore, the number of times that mutations for CCR2 are found do not exceed 3 patients out of ~13 000 patients screened. As these mutants could clearly affect receptor functionality and drugability, it is necessary to increase attention to obtain a larger sample size. Interestingly, CCR2 have been described to form heterodimers with multiple (non-chemokine receptor) GPCRs [49]. Mutations could conceivably interfere with dimer formation and functioning. Of note, it is unclear why the studied mutations in this research all negatively impacted receptor activation. Increased expression and activation of CCR2 promotes cancer progression based on increased expression and the receptor's function [6,7], but examined mutations suggest an opposite role. Hence, experiments focusing on cell morphology, migration and proliferation of mutants in CCR2-expressing cancer cell lines could further clarify the role of CCR2 mutants in cancer. In conclusion, the cancer-associated mutations of CCR2 studied in this paper negatively affected its activation by CCL2. This could affect cancer-related processes such as metastasis, proliferation and immunosuppression, in which CCR2 plays a big role. This finding invites further research of the role of CCR2 mutations in proliferation and migration using cancer cell lines. In addition, several mutants showed a loss of orthosteric and/or antagonist binding, which could prove a hurdle for CCR2-based cancer treatment. Since CCR2 is seen as a promising cancer drug target, it has to be acknowledged that cancer-associated mutations need to be considered when targeting this receptor with small molecule antagonists.

## CRediT authorship contribution statement

**L.S. den Hollander:** Conceptualization, Methodology, Investigation, Formal analysis, Data curation, Writing – original draft, Visualization. **O.J.M. Béquignon:** Methodology, Investigation, Software, Visualization. **X. Wang:** Methodology. **K. van Wezel:** Investigation. **J. Broekhuis:** Investigation. **M. Gorostiola González:** Investigation. **K.E. de Visser:** Writing – review & editing. **A.P. IJzerman:** Writing – review & editing, Supervision. **G.J.P. van Westen:** Writing – review & editing, Supervision. **L.H. Heitman:** Conceptualization, Writing – review & editing, Supervision, Project administration, Funding acquisition.

## Declaration of Competing Interest

The authors declare that they have no known competing financial interests or personal relationships that could have appeared to influence the work reported in this paper.

## Data availability

Data will be made available on request.

## Acknowledgments

This publication is financed by the Dutch Research Council (NWO) (#16573).

## References

[1] H. Sung, J. Ferlay, R.L. Siegel, M. Laversanne, I. Soerjomataram, A. Jemal, F. Bray, Global Cancer Statistics 2020: GLOBOCAN Estimates of Incidence and Mortality Worldwide for 36 Cancers in 185 Countries, CA: Cancer, J. Clin. 71 (3) (2021) 209–249.
[2] N. Arang, J.S. Gutkind, G Protein-Coupled receptors and heterotrimeric G proteins as cancer drivers, FEBS Letters 594 (24) (2020) 4201–4232.
[3] S. Usman, M. Khawer, S. Rafique, Z. Naz, K. Saleem, The current status of anti-GPCR drugs against different cancers, J. Pharm. Anal. 10 (6) (2020) 517–521.
[4] C.E. Hughes, R.J.B. Nibbs, A guide to chemokines and their receptors, FEBS J. 285 (16) (2018) 2944–2971.
[5] R.A. Lacalle, R. Blanco, L. Carmona-Rodríguez, A. Martín-Leal, E. Mira, S. Mañes, Chemokine Receptor Signaling and the Hallmarks of Cancer, Int. Rev. Cell Mol. Biol. 331 (2017) 181–244.
[6] M. Xu, Y. Wang, R. Xia, Y. Wei, X. Wei, Role of the CCL2-CCR2 signalling axis in cancer: Mechanisms and therapeutic targeting, Cell Prolif. 54 (10) (2021) e13115.
[7] N. Nagarsheth, M.S. Wicha, W. Zou, Chemokines in the cancer microenvironment and their relevance in cancer immunotherapy, Nat. Rev. Immunol. 17 (9) (2017) 559–572.
[8] X.W. Zhang, X. Qin, C.Y. Qin, Y.L. Yin, Y. Chen, H.L. Zhu, Expression of monocyte chemoattractant protein-1 and CC chemokine receptor 2 in non-small cell lung cancer and its significance, Cancer Immunol. Immunother. 62 (3) (2013) 563–570.
[9] N.V. Ortiz Zacarías, M.P. Bemelmans, T.M. Handel, K.E. de Visser, L.H. Heitman, Anticancer opportunities at every stage of chemokine function, Trends Pharmacol. Sci. 42 (11) (2021) 912–928.
[10] L. Fei, X. Ren, H. Yu, Y. Zhan, Targeting the CCL2/CCR2 Axis in Cancer Immunotherapy: One Stone, Three Birds? Front. Immunol. 12 (2021), 771210.
[11] G. Soria, A. Ben-Baruch, The inflammatory chemokines CCL2 and CCL5 in breast cancer, Cancer Lett. 267 (2) (2008) 271–285.
[12] L. Li, Y. Liu, Y. Zhan, Y. Zhu, Y. Li, D. Xie, X. Guan, High levels of CCL2 or CCL4 in the tumor microenvironment predict unfavorable survival in lung adenocarcinoma, Thorac. Cancer 9 (7) (2018) 775–784.
[13] M. Ohta, Y. Kitadai, S. Tanaka, M. Yoshihara, W. Yasui, N. Mukaida, K. Haruma, K. Chayama, Monocyte chemoattractant protein-1 expression correlates with macrophage infiltration and tumor vascularity in human gastric carcinomas, Int. J. Oncol. 22 (4) (2003) 773–778.
[14] N. V. Ortiz Zacarías, E. B. Lenselink, A. P. IJzerman, T. M. Handel, L. H. Heitman, Intracellular Receptor Modulation: Novel Approach to Target GPCRs, Trends Pharmacol. Sci. 39(6) (2018) 547–559.
[15] Y. Zheng, L. Qin, N.V. Ortiz Zacarías, H. de Vries, G. Won Han, M. Gustavsson, M. Dabros, C. Zhao, R.J. Cherney, P. Carter, D. Stamos, R. Abagyan, V. Cherezov, R.C. Stevens, A.P. IJzerman, L.H. Heitman, A. Tebben, I. Kufareva, T.M. Handel, Structure of CC Chemokine Receptor 2 with Orthosteric and Allosteric Antagonists, Nature 540 (2016) 458–461.
[16] A. Apel, R.K.Y. Cheng, C.S. Tautermann, M. Brauchle, C. Huang, A. Pautsch, M. Hennig, H. Nar, G. Schnapp, Crystal Structure of CC Chemokine Receptor 2A in Complex with an Orthosteric Antagonist Provides Insights for the Design of Selective Antagonists, Structure 27 (3) (2019) 427–438.
[17] K. Jaeger, S. Bruenle, T. Weinert, W. Guba, J. Muehle, T. Miyazaki, M. Weber, A. Furrer, N. Haenggi, T. Tetaz, C. Huang, D. Mattle, J. Vonach, A. Gast, A. Kuglstatter, M.G. Rudolph, P. Nogly, J. Benz, R.J.P. Dawson, J. Standfuss, Structural Basis for Allosteric Ligand Recognition in the Human CC Chemokine Receptor 7, Cell 178 (5) (2019) 1222–1230.
[18] C. Oswald, M. Rappas, J. Kean, A.S. Doré, J.C. Errey, K. Bennett, F. Deflorian, J. A. Christopher, A. Jazayeri, J.S. Mason, M. Congreve, R.M. Cooke, F.H. Marshall, Intracellular allosteric antagonism of the CCR9 receptor, Nature 540 (2016) 462–465.
[19] K. Liu, L. Wu, S. Yuan, M. Wu, Y. Xu, Q. Sun, S. Li, S. Zhao, T. Hua, Z. Liu, Structural basis of CXC chemokine receptor 2 activation and signalling, Nature 585 (2020) 135–140.
[20] O.A. Dasse, J.L. Evans, H. Zhai, D. Zou, J.T. Kintigh, F. Chan, K. Hamilton, E. Hill, J.B. Eckman, P.J. Higgins, A. Volosov, P. Collart, J.-M. Nicolas, R.K. Kondru, C. E. Schwartz, Novel, Acidic CCR2 Receptor Antagonists: Lead Optimization, Lett. Drug Des. Discov. 4 (4) (2008) 263–271.
[21] M. O'Hayre, J. Vázquez-Prado, I. Kufareva, E.W. Stawiski, T.M. Handel, S. Seshagiri, J.S. Gutkind, The emerging mutational landscape of G proteins and G-protein-coupled receptors in cancer, Nat. Rev. Cancer 13 (6) (2013, 2013,) 412–424.
[22] J.N. Weinstein, E.A. Collisson, G.B. Mills, K.R. Mills Shaw, B.A. Ozenberger, K. Ellrott, I. Shmulevich, C. Sander, J.M. Stuart, The cancer genome atlas pan-cancer analysis project, Nat. Genet. 45 (10) (2013) 1113–1120.
[23] X. Wang, W. Jespers, B.J. Bongers, M.C.C. Habben Jansen, C. M. Stangenberger, M. A.Dilweg, H. Gutiérrez-de-Terán, A.P. IJzerman, L.H. Heitman, G.J.P. van Westen, Characterization of cancer-related somatic mutations in the adenosine A2B receptor, Eur. J. Pharmacol. 880 (2020) 173126.
[24] C. Ierano, P. Giuliano, C. D'Alterio, M. Cioffi, V. Mettivier, L. Portella, M. Napolitano, A. Barbieri, C. Arra, G. Liguori, R. Franco, G. Palmieri, C. Rozzo, R. Pacelli, G. Castello, S. Scala, A point mutation (G574A) in the chemokine

receptor CXCR4 detected in human cancer cells enhances migration, Cell Cycle 8 (8) (2009) 1228–1237.
[25] F. Maestro, Schrödinger Release 2020–1, Schrödinger, LLC, New York, NY, 2021.
[26] E.F. Pettersen, T.D. Goddard, C.C. Huang, G.S. Couch, D.M. Greenblatt, E.C. Meng, T.E. Ferrin, UCSF Chimera - A visualization system for exploratory research and analysis, J. Comput. Chem. 25 (13) (2004) 1605–1612.
[27] H. Nomiyama, O. Yoshie, Functional roles of evolutionary conserved motifs and residues in vertebrate chemokine receptors, J. Leukoc. Biol 97 (1) (2015) 39–47.
[28] C.M. Brodmerkel, R. Huber, M. Covington, S. Diamond, L. Hall, R. Collins, L. Leffet, K. Gallagher, P. Feldman, P. Collier, M. Stow, X. Gu, F. Baribaud, N. Shin, B. Thomas, T. Burn, G. Hollis, S. Yeleswaram, K. Solomon, S. Friedman, A. Wang, C. Biao Xue, R.C. Newton, P. Scherle, K. Vaddi, Discovery and Pharmacological Characterization of a Novel Rodent-Active CCR2 Antagonist, INCB3344, J. Immunol. 175 (8) (2005) 5370–5378.
[29] N.V. Ortiz Zacarías, K.K. Chahal, T. Šimková, C. van der Horst, Y. Zheng, A. Inoue, E. Theunissen, L. Mallee, D. van der Es, J. Louvel, A.P. IJzerman, T.M. Handel, I. Kufareva, L.H. Heitman, Design and characterization of an intracellular covalent ligand for cc chemokine receptor 2, J. Med. Chem. 64(5) (2021) 2608−2621.
[30] N.V. Ortiz Zacarías, J.P.D. van Veldhoven, L. Portner, E. van Spronsen, S. Ullo, M. Veenhuizen, W.J.C. van der Velden, A.J.M. Zweemer, R.M. Kreekel, K. Oenema, E.B. Lenselink, L.H. Heitman, A.p., IJzerman, Pyrrolone Derivatives as Intracellular Allosteric Modulators for Chemokine Receptors: Selective and Dual-Targeting Inhibitors of CC Chemokine Receptors 1 and 2, J. Med. Chem. 61 (20) (2018) 9146–9161.
[31] P.K. Smith, R.I. Krohn, G.T. Hermanson, A.K. Mallia, F.H. Gartner, M. D. Provenzano, E.K. Fujimoto, N.M. Goeke, B.J. Olson, D.C. Klenk, Measurement of Protein Using Bicinchoninic Acid, Anal. Biochem. 1 (150) (1985) 76–85.
[32] R. Abagyan, M. Totrov, D. Kuznetsov, ICM—A new method for protein modeling and design: Applications to docking and structure prediction from the distorted native conformation, J. Comput. Chem. 15 (5) (1994) 488–506.
[33] M.A.C. Neves, M. Totrov, R. Abagyan, Docking and scoring with ICM: The benchmarking results and strategies for improvement, J. Comput. Aided Mol. Des. 26 (6) (2012) 675–686.
[34] H. Nomiyama, O. Yoshie, Functional roles of evolutionary conserved motifs and residues in vertebrate chemokine receptors, J. Leukoc. Biol. 97(1) (2015) 39–47, 2015.
[35] E.C. Hulme, GPCR activation: A mutagenic spotlight on crystal structures, Trends Pharmacol. Sci. 34 (1) (2013) 67–84.
[36] B.J. Bongers, M. Gorostiola González, X. Wang, H.W.T. van Vlijmen, W. Jespers, H. Gutiérrez-de-Terán, K. Ye, A.P. IJzerman, L.H. Heitman, G.J.P. van Westen, Pan-cancer in silico analysis of somatic mutations in G-protein coupled receptors: The effect of evolutionary conservation and natural variance, (2021). (*preprint*).
[37] Z. Shao, Y. Tan, Q. Shen, L. Hou, B. Yao, J. Qin, P. Xu, C. Mao, L. Chen, H. Zhang, D. Shen, C. Zhang, W. Li, X. Du, F. Li, Z. Chen, Y. Jiang, H.E. Xu, S. Ying, H. Ma, Y. Zhang, H. Shen, Molecular insights into ligand recognition and activation of chemokine receptors CCR2 and CCR3, Cell Discov. 8 (2022) 44.
[38] A.J. Venkatakrishnan, X. Deupi, G. Lebon, C.G. Tate, G.F. Schertler, M. Madan Babu, Molecular signatures of G-protein-coupled receptors, Nature 494 (2013) 185–194.
[39] A. Scheer, F. Fanelli, T. Costa, P.G. De Benedetti, S. Cotecchia, The activation process of the α1B-adrenergic receptor: Potential role of protonation and hydrophobicity of a highly conserved aspartate, Proc. Natl. Acad. Sci. USA 94 (3) (1997) 808–813.
[40] J. Ballesteros, S. Kitanovic, F. Guarnieri, P. Davies, B.J. Fromme, K. Konvicka, L. Chi, R.P. Millar, J.S. Davidson, H. Weinstein, S.C. Sealfon, Functional microdomains in G-protein-coupled receptors: The conserved arginine-cage motif in the gonadotropin-releasing hormone receptor, J. Biol. Chem. 273 (17) (1998) 10445–10453.
[41] S.G. Rasmussen, A.D. Jensen, G. Liapakis, P. Ghanouni, J.A. Javitch, U. Gether, Mutation of a highly conserved aspartic acid in the β2 adrenergic receptor: Constitutive activation, structural instability, and conformational rearrangement of transmembrane segment 6, Mol. Pharmacol. 56 (1) (1998) 175–184.
[42] G.E. Rovati, V. Capra, R.R. Neubig, The highly conserved DRY motif of class A G protein-coupled receptors: Beyond the ground state, Mol. Pharmacol. 71 (4) (2007) 959–964.
[43] G.A. Auger, J.E. Pease, X. Shen, G. Xanthou, M.D. Barker, Alanine scanning mutagenesis of CCR3 reveals that the three intracellular loops are essential for functional receptor expression, Eur. J. Immunol. 32 (4) (2002) 1052–1058.
[44] B. Lagane, S. Ballet, T. Planchenault, K. Balabanian, E. Le Poul, C. Blanpain, Y. Percherancier, I. Staropoli, G. Vassart, M. Oppermann, M. Parmentier, F. Bachelerie, Mutation of the DRY Motif Reveals Different Structural Requirements for the CC Chemokine Receptor 5-Mediated Signaling and Receptor Endocytosis, Mol. Pharmacol. 67 (6) (2005) 1966–1976.
[45] A. de Voux, M.C. Chan, A.T. Folefoc, M.T. Madziva, C.A. Flanagan, Constitutively Active CCR5 Chemokine Receptors Differ in Mediating HIV Envelope-dependent Fusion, PLoS ONE 8 (1) (2013) e54532.
[46] X. Han, Y. Feng, X. Chen, C. Gerard, W.A. Boisvert, Characterization of G protein coupling mediated by the conserved $D134^{3.49}$ of DRY motif, $M241^{6.34}$, and $F251^{6.44}$ residues on human CXCR1, FEBS Open Bio 5 (2015) 182–190.
[47] A.J.M. Zweemer, I. Nederpelt, H. Vrieling, S. Hafith, M.L.J. Doornbos, H. de Vries, J. Abt, R. Gross, D. Stamos, J. Saunders, M.J. Smit, A.P. IJzerman, L.H. Heitman, Multiple Binding Sites for Small-Molecule Antagonists at the CC Chemokine Receptor 2, Mol. Pharmacol. 84(4) (2013) 551–561.
[48] A.J.M. Zweemer, J. Bunnik, M. Veenhuizen, F. Miraglia, E.B. Lenselink, M. Vilums, H. de Vries, A. Gibert, S. Thiele, M.M. Rosenkilde, A.P. IJzerman, L.H. Heitman, Discovery and Mapping of an Intracellular Antagonist Binding Site at the Chemokine Receptor CCR2, Mol Pharmacol. 86(4) (2014) 358–368.
[49] I. Gomes, M.A. Ayoub, W. Fujita, W.C. Jaeger, K.D.G. Pfleger, L.A. Devi, G Protein-Coupled Receptor Heteromers, Annu. Rev. Pharmacol. Toxicol. 56 (2016) 403–425.